BIOCHEMISTRY
including biophysical chemistry & molecular biology

Article

pubs.acs.org/biochemistry

A New Type of Dual-Cys Cyanobacteriochrome GAF Domain Found in Cyanobacterium *Acaryochloris marina*, Which Has an Unusual Red/Blue Reversible Photoconversion Cycle

Rei Narikawa,*[,†,‡,§] Gen Enomoto,[†] Ni-Ni-Win,[†] Keiji Fushimi,[‡] and Masahiko Ikeuchi[†,∥]

[†]Department of Life Sciences (Biology), Graduate School of Arts and Sciences, University of Tokyo, Komaba 3-8-1, Meguro, Tokyo 153-8902, Japan

[‡]Department of Biological Science, Faculty of Science, Shizuoka University, Suruga-ku, Shizuoka 422-8529, Japan

[§]PRESTO, Japan Science and Technology Agency (JST), 4-1-8 Honcho Kawaguchi, Saitama 332-0012, Japan

[∥]CREST, Japan Science and Technology Agency (JST), 4-1-8 Honcho Kawaguchi, Saitama 332-0012, Japan

Supporting Information

ABSTRACT: Cyanobacteriochromes (CBCRs) form a large, spectrally diverse family of photoreceptors (linear tetrapyrrole covalently bound via a conserved cysteine) that perceive ultraviolet to red light. The underlying mechanisms are reasonably well understood with, in certain cases, reversible formation of an adduct between a second cysteine and the chromophore accounting, in part, for their spectral diversity. These CBCRs are denoted as dual-Cys CBCRs, and most such CBCRs had been shown to reversibly absorb blue and green light. Herein, we report the structural and mechanistic characterization of a new type of dual-Cys CBCR, AM1_1186, which exhibits reversible photoconversion between a red-absorbing dark state (λ_{max} = 641 nm) and a blue-absorbing photoproduct (λ_{max} = 416 nm). The wavelength separation of AM1_1186 photoconversion is the largest found to date for a CBCR. In addition to one well-conserved cysteine responsible for covalent incorporation of the chromophore into the apoprotein, AM1_1186 contains a second cysteine in a unique position of its photosensory domain, which would be more properly classified as a red/green CBCR according to its sequence. Carboxyamidomethylation and mutagenesis of the cysteines revealed that the second cysteine forms an adduct with the tetrapyrrole, the phycocyanobilin, that can be reversed under blue light. The proline immediately upstream of this cysteine appears to determine the rate at which the cysteinylation following photoexcitation of the dark state chromophore can occur. We propose a possible reaction scheme and color-tuning mechanism for AM1_1186 in terms of its structure and its place in a phylogenetic tree.

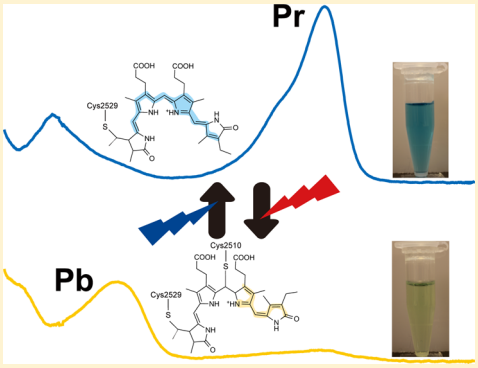

Phytochromes are photosensory proteins containing a linear tetrapyrrole type chromophore that absorbs red and far-red light to regulate a wide range of physiological processes in bacteria, fungi, algae, and plants.[1−3] Their N-terminal photosensory modules contain Per/ARNT/Sim, GAF (cGMP-phosphodiesterase/adenylate cyclase/FhlA), and phytochrome-specific domains.[3−5] A canonical cysteine residue irreversibly ligates to the chromophore. Light irradiation triggers a *Z*/*E* isomerization of the C15═C16 bond between pyrrole rings C and D. Recently, certain cyanobacterial and algal phytochromes have been found to exhibit photoconversions not typically seen for phytochromes; i.e., they sense blue, green, or orange light.[6,7]

CBCRs are photoreceptors that are distantly related to the phytochromes,[8] and only a GAF domain is needed for chromophore binding and photoconversion, unlike the case for phytochromes. A canonical Cys residue within the GAF domain covalently ligates to the chromophore. To date, CBCRs have been found only in cyanobacteria and sense near-ultraviolet (UV) and visible light to regulate chromatic acclimation of phycobiliproteins and the phototactic orientation of cells.[9−13] *Z*/*E* isomerization of the C15═C16 bond between rings C and D of the tetrapyrrole moiety occurs during CBCR photoconversion as it does in phytochromes.

The spectral diversity of CBCRs is a consequence of their distinct color-tuning mechanisms, involving the apoprotein and the specific tetrapyrrole moiety. Cys-based spectral recognition, i.e., the reversible binding of a cysteine thiol to the tetrapyrrole chromophore, is one of the most common color-tuning mechanisms across the subfamilies. We denote herein CBCRs that require two cysteines for function (one for irreversible binding of the chromophore and the second for reversible binding) as dual-Cys CBCRs. For these CBCRs, in addition to a canonical Cys that is irreversibly bound to the chromophore, a second conserved cysteine reversibly binds the chromophore. This reaction is responsible for the observed spectral shifts.

Received: March 28, 2014
Revised: June 27, 2014
Published: July 16, 2014

   dx.doi.org/10.1021/bi500376b | *Biochemistry* 2014, 53, 5051−5059

Blue/green (B/G) CBCRs are representative of such dual-Cys CBCRs. Most B/G CBCRs covalently bind phycoviolobilin (PVB) and reversibly photoconvert between a blue light-absorbing (B) dark state (15*Z*, Pb) and a green light-absorbing (G) photoproduct (15*E*, Pg).[10,11,14−20] A cysteine within a conserved DXCF motif in the GAF domain of B/G CBCRs is responsible for the reversible binding to the chromophore during photoconversion.[15,16,21,22] Structural determination of TePixJg, a B/G CBCR, which is involved in the phototactic orientation of cells, clearly shows that the second cysteine is covalently bound to C10 of the chromophore in its Pb dark state and is free in the Pg photoproduct.[23−25] Recent comprehensive analyses revealed that many variants in their functioning exist within the B/G CBCR subfamily.[11,14,15,21] Although the blue light-absorbing Cys adduct form of B/G CBCRs is usually the dark state and has a 15*Z* chromophore, one B/G CBCR GAF domain, NpR5313g2, has a blue light-absorbing Cys adduct form for its photoproduct. In addition to B/G CBCRs with the second cysteine located in the DXCF motif, CBCRs from other subfamilies and phytochromes with Cys-based spectral recognition have been identified.[7,26] These CBCRs, VO1 and UB1 (named insert-Cys CBCRs), contain a second Cys that is not located in a DXCF motif, but in an inserted sequence instead, and is responsible for the reversible or stable binding/photoconversion process.

Red/green (R/G) CBCRs adopt a color-tuning mechanism distinct from Cys-based recognition. R/G CBCRs, represented by AnPixJg2, covalently bind phycocyanobilin (PCB) and reversibly photoconvert between a red light-absorbing (R) dark state (15*Z*, Pr) and a green light-absorbing (G) photoproduct (15*E*, Pg) without the involvement of a second cysteine.[27−32] For these CBCRs, the Pr dark state is almost same as that of the phytochrome Pr dark state, and its photoconversion is initiated by a *Z*/*E* isomerization similar to that of phytochromes, but the Pg photoproduct is different.[27,29,31,33] Recently, we determined the crystal structure of the AnPixJg2 Pr dark state.[24,34] Its chromophore and tertiary structures are quite similar to those of the phytochrome Pr dark states. The AnPixJg2 Pr structure validates that conserved residues (Asp291 and Trp289) are important for the structural change that occurs upon red light illumination for the formation of the Pg photoproduct.[24,33] Hydration and ring D distortion may also occur during Pr-to-Pg photoconversion, although the reaction(s) resulting in AnPixJg2 Pg formation remains to be unraveled.[33,35]

For this study, we characterized the unusual dual-Cys CBCR GAF domain AM1_1186g2 from the cyanobacterium *Acaryochloris marina* MBIC11017. Although AM1_1186g2 might be categorized as an R/G CBCR according to its primary sequence, it reversibly photoconverts between a red light-absorbing Pr dark state and a blue light-absorbing Pb photoproduct instead. Using iodoacetamide (IAM) to alkylate cysteines and site-directed mutagenesis of cysteines, we show that a cysteine not previously implicated in photoconversion of CBCRs binds PCB in AM1_1186g2 Pb but not in Pr, as found for B/G CBCRs. These results indicate that the structural plasticity and evolutionary flexibility of CBCRs are much larger than previously thought.

EXPERIMENTAL PROCEDURES

***In Silico* Characterization of AM1_1186 and AM1_1186g2.** The composition of the AM1_1186 domain was determined using SMART (http://smart.embl-heidelberg.de/).[36] Multiple-sequence alignment and phylogenetic clustering of AM1_1186g2 were performed with CLUSTAL_X.[37] The phylogenetic tree and structures were drawn by Dendroscope[38] and PyMOL (http://pymol.org), respectively.

Plasmid Construction. *Escherichia coli* strain JM109 (Novagen) was used for plasmid construction. Cells were grown in Luria-Bertani medium with 20 μg/mL kanamycin. The DNA fragment corresponding to AM1_1186g2 was obtained by polymerase chain reaction (PCR) amplification of genomic DNA from the cyanobacterium *A. marina* MBIC11017 with the use of primers 5′-CGCGGCAGCCATATGGCACTCAATCGGATCACC-3′ and 5′-CTCGAATTCGGATCCTCACGCATCGGCTTTTTCTTT-3′. Linearized pET28a (Novagen, Madison, WI) was generated by PCR amplification with primers 5′-CATATGGCTGCCGCGCGG-3′ and 5′-GGATCCGAATTCGAGCTC-3′ and pET28a plasmid DNA. AM1_1186g2 was cloned into pET28a using the In-Fusion system (TaKaRa, Ohtsu, Japan), and the resulting plasmid was designated pET28a_AM1_1186g2.

To introduce mutations into AM1_1186g2 in which the codons encoding cysteines at positions 2460 and 2580 were each replaced with codons encoding alanines, two DNA fragments were amplified with primer sets of 5′-CTGGGGGCCGAACGGGTAACGGTCTA-3′ and 5′-TGACTGGCGACCTGTTCAAATAGCCT-3′, and 5′-CCGTTCGGCCCCCAGAATGGGTCTGAC-3′ and 5′-ACAGGTCGCCAGTCATTTAGGCGTTGC-3′, and PrimeSTAR Max DNA polymerase (TaKaRa) from wild type plasmid pET28a_AM1_1186g2. The two fragments were fused using the In-Fusion system, and the resulting plasmid was denoted pET28a_AM1_1186g2_CCAA.

To introduce a mutation into AM1_1186g2 in which the codon encoding the cysteine at position 2510 was replaced with a codon encoding an alanine, a DNA fragment was amplified using a primer set of 5′-AATCCCGCCGTATTTAACACCACTTAT-3′ and 5′-AAATACGGCGGGATTCCCCTCTTCGTT-3′ and PrimeSTAR Max DNA polymerase from wild type plasmid pET28a_AM1_1186g2, and the mutated plasmid was obtained using PrimeSTAR Max mutagenesis kit reagents (TaKaRa). The resulting plasmid was denoted pET28a_AM1_1186g2_CA. pET28a_AM1_1186g2_PA, in which the codon encodes the proline at position 2509 in AM1_1186, was obtained in the same way as described above with a primer set of 5′-GGGGAATGCCTGTGTATTTAACACCA-3′ and 5′-ACACAGGCATTCCCCTCTTCGTTGAC-3′. The sequences of the genes encoding AM1_1186g2 and its mutants were verified.

Expression and Purification of His-Tagged AM1_1186g2 and Its Mutants. *E. coli* strain C41 (Novagen) carrying pKT271[39] for the production of PCB was used for expression of AM1_1186g2, AM1_1186g2_CCAA, AM1_1186g2_CA, and AM1_1186g2_PA. Each culture was incubated at 37 °C for 2.5 h in 1 L of Luria-Bertani medium, 20 μg/mL kanamycin, and 20 μg/mL chloramphenicol, after which isopropyl thio-β-D-galactopyranoside was added to a final concentration of 0.1 mM. Next, the cells were cultured at 18 °C overnight and then harvested by centrifugation. Each cell pellet was frozen at −80 °C, thawed at 4 °C, suspended in 50 mL of 20 mM HEPES-NaOH (pH 7.5), 100 mM NaCl, and 10% (w/v) glycerol (buffer A), and disrupted by three passages through an Emulsifies C5 high-pressure homogenizer at 12000 psi (Avestin, Ottawa, ON). The lysate was centrifuged at 109200*g* for 30 min at 4 °C, and the supernatant containing His-tagged protein was passed through a nickel affinity His-trap chelating column (GE Healthcare, Piscataway, NJ). After being washed

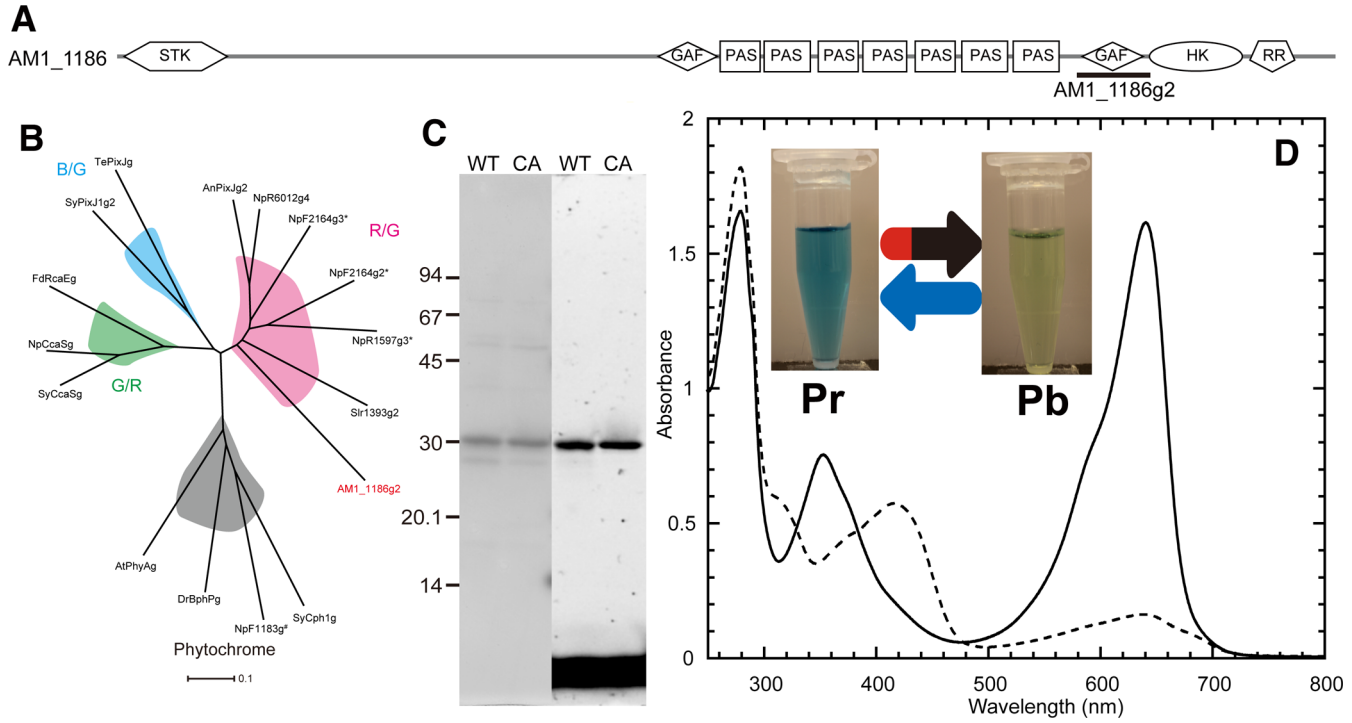

Figure 1. (A) AM1_1186 domain architecture determined by SMART (http://smart.embl-heidelberg.de/). (B) Phylogenetic cluster of R/G, G/R, B/G, and insert-Cys CBCR GAF and phytochrome GAF domains. AM1_1186g2 is shown in red type. The insert-Cys CBCR and the dual-Cys phytochrome domains are marked with an asterisk and a number sign, respectively. (C) SDS−PAGE and zinc fluorescence assay of His-tagged AM1_1186g2 (WT) and AM1_1186g2_CA (CA) purified from PCB-producing *E. coli*. CBB staining (left) and fluorescence (right) after soaking of the gel in zinc acetate. (D) Absorption spectra of AM1_1186g2 Pr (—) and Pb (---). Insets are photographs of solutions containing AM1_1186g2 Pr and Pb.

with 30 mM imidazole in buffer A, the column was washed with a step gradient of 50, 100, and 200 mM imidazole in buffer A. The His-tagged proteins were recovered in the 200 mM imidazole fraction, which was then dialyzed against buffer A to remove the imidazole.

Sodium Dodecyl Sulfate−Polyacrylamide Gel Electrophoresis (SDS−PAGE) and Zinc-Dependent Fluorescence Gel Assay. Isolated proteins were solubilized in 2% (w/v) lithium dodecyl sulfate, 60 mM dithiothreitol, and 60 mM Tris-HCl (pH 8.0) and subjected to SDS−PAGE through a 15% (w/v) polyacrylamide gel, which was then stained with Coomassie Brilliant Blue R-250. For the zinc-dependent fluorescence assay, after SDS−PAGE of the His-tagged fraction, the gel was soaked in 20 μM zinc acetate at room temperature for 30 min in the dark.[40] Then fluorescence was visualized using a fluorescence detection system (FMBIO II, TaKaRa). Emission excited with 532 nm light was detected through a 605 nm filter.

Spectrometry. Ultraviolet and visible absorbance spectra of all proteins were recorded using a model UV-2600 spectrophotometer (Shimadzu, Kyoto, Japan) at room temperature. Red light was provided by a light-emitting diode with a peak wavelength of 639 nm and a 20 nm half-bandwidth. A light-emitting diode with a peak wavelength of 400 nm and a 15 nm half-bandwidth provided blue light. After the proteins had been denatured in 8 M urea (pH 2.0) in the dark, their absorbance spectra were measured also in the dark and then recorded again after white light irradiation for 3 min. For irreversible chemical modification of cysteine thiols, IAM was added to each protein solution at a final concentration of 50 mM, and the mixtures were then incubated for 60 min at room temperature in the dark as previously reported.[41]

RESULTS AND DISCUSSION

Sequence Characteristics of AM1_1186g2. AM1_1186 is a large protein (3073 residues) that contains an N-terminal Ser/Thr kinase domain, followed by a long conserved region of unknown function, a non-CBCR GAF domain, seven Per/ARNT/Sim domains, one CBCR type GAF domain (AM1_1186g2), one His-kinase domain, and one response regulator domain at its C-terminus (Figure 1A). AM1_1186g2 is a member of the R/G CBCR subfamily according to our multisequence alignment (Figure 1 of the Supporting Information) and phylogenetic clustering (Figure 1B). It contains residues that are uniquely conserved among R/G CBCRs (Figure 1 of the Supporting Information).

AM1_1186g2 Exhibits an Unusual Reversible Red/Blue Photoconversion. His-tagged AM1_1186g2 expressed in a PCB-producing *E. coli* was purified to near homogeneity and covalently bound a linear tetrapyrrole judging from strong zinc-dependent fluorescence (Figure 1C). AM1_1186g2 reversibly photoconverted between Pr with an absorbance maximum at 641 nm and Pb with an absorbance maximum at 416 nm (Figure 1D). The spectrum of AM1_1186g2 Pb is markedly blue-shifted (~130 nm) in comparison with that of AnPixJg2 Pg, whereas the spectra of the two corresponding Pr states are very similar.[27] Notably, photoconversion from AM1_1186g2 Pr to Pb occurs in two steps (Figure 2A). Red light irradiation of Pr causes the transient formation of an intermediate (Io) with an absorbance maximum at 617 nm. This species slowly decays to form Pb. To measure the kinetics

dx.doi.org/10.1021/bi500376b | *Biochemistry* 2014, 53, 5051−5059

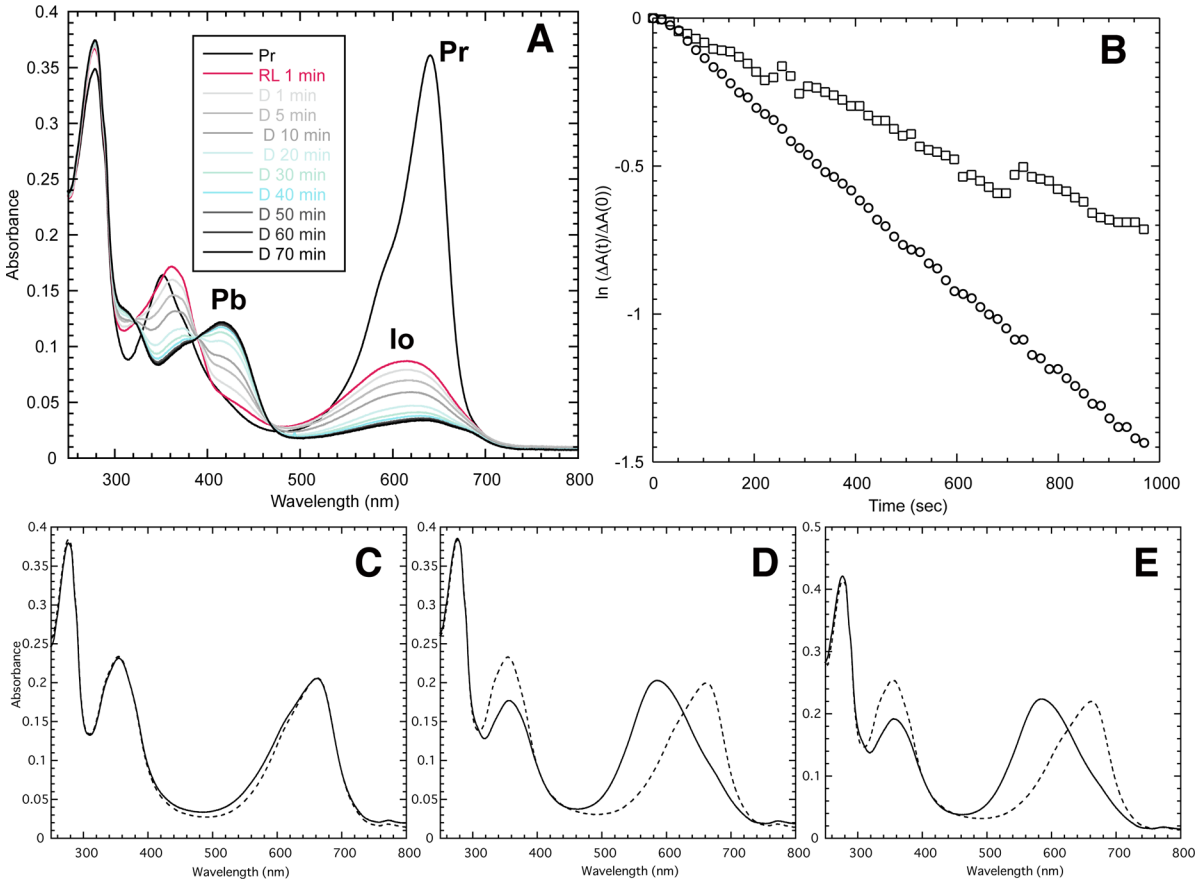

Figure 2. (A) Pr-to-Pb photoconversion of AM1_1186g2. The Pr-to-Pb photoconversion occurs in two steps: Pr to Io and then Io to Pb. Spectra of a Pr solution before red light irradiation (Pr), after red light irradiation for 1 min for Pr-to-Io photoconversion ("RL 1 min") and for 1−70 min after red light irradiation recorded in the dark ("D 1, 5···70 min"). (B) Kinetics of AM1_1186g2 Io-to-Pb conversion measured at 30 °C (○) and 20 °C (□) under the dark condition. The absorbance at 416 nm was monitored. Spectra of acid-denatured AM1_1186g2 (C) Pr, (D) Io, and (E) Pb. Spectra were recorded immediately after denaturation (—) and then after white light illumination (---).

of Io-to-Pb conversion, we monitored the absorbance at 416 nm at 30 and 20 °C in the dark (○ and □, respectively, in Figure 2B). Semilogarithmic plots of the Io-to-Pb transition at the two temperatures are linear, indicating that the transition is a first-order reaction (Figure 2B). The half-lives at 30 and 20 °C are 486 and 988 s, respectively. This temperature-dependent dark reaction seems to be rate-limiting in the reaction from Pr to Pb. Conversely, irradiation of Pb with blue light quickly regenerated Pr without a noticeable accumulation of an intermediate.

Chromophore Species and Configurations. To determine the type of chromophore and its configuration, acid-denatured spectra of Pr, Io, and Pb were acquired. An absorbance peak in the spectrum of denatured Pr is present at 661 nm and unaffected by white light illumination (Figure 2C), indicating that Pr harbors the C15-*Z* isomer of PCB and is the dark state. Conversely, the absorbance peaks of denatured Io and Pb at 598 nm were red-shifted to 661 nm upon being irradiated with white light (panels D and E of Figure 2, respectively), indicating that Io and Pb harbor a C15-*E* PCB and that Pb is the photoproduct. Therefore, upon red light illumination, Pr quickly photoconverts to Io via a *Z*/*E* isomerization of the C15═C16 bond, which is followed by a slow conversion to Pb in the dark.

Formation of a Reversible Covalent Bond Involving Cys2510 and PCB. We hypothesized that upon formation of AM1_1186g2 Pb a covalent bond between a cysteine and C10 of PCB had formed in a reaction similar to that of B/G CBCRs. To verify this hypothesis, we subjected AM1_1186g2 in its Pr and Pb forms to IAM alkylation (Figure 3). Incubation of Pr with IAM resulted in no obvious changes in its spectrum. When Pr was irradiated with red light in the presence of IAM, Io formed, and the amount of Pr decreased concomitantly (Figure 3A). However, this modified Io was stable and did not convert in the dark to Pb within 10 min (Figure 3A), clearly indicating that the formation of Pb involved a covalent bond between a cysteine and PCB.

Conversely, addition of IAM to Pb in the dark resulted in the slow partial production of Io with a concomitant decrease in the amount of Pb present (Figure 3B). Blue light irradiation of IAM-incubated Pb resulted in the formation of Pr, indicating that Pr formation does not require a free cysteine. It is not clear whether Io was also photoconverted to Pr. Regardless, following red light irradiation of IAM-incubated Pr resulted in Io formation but not in Pb formation in the dark (Figure 3B). These results demonstrate that AM1_1186g2 undergoes a thiol-based photocycle involving a Cys-free Pr state and a Cys adduct Pb state. We assume that the slow partial conversion of Pb to Io after IAM treatment reflects the modification of a small amount of free cysteine, which is present in equilibrium with the Cys adduct Pb. A similar equilibrium process was observed for the Tlr1999 photoconversion in the presence of IAM.[15]

AM1_1186g2 contains four cysteines [Cys2460, Cys2510, Cys2529, and Cys2580 (Figure 1 of the Supporting

dx.doi.org/10.1021/bi500376b | *Biochemistry* 2014, 53, 5051−5059

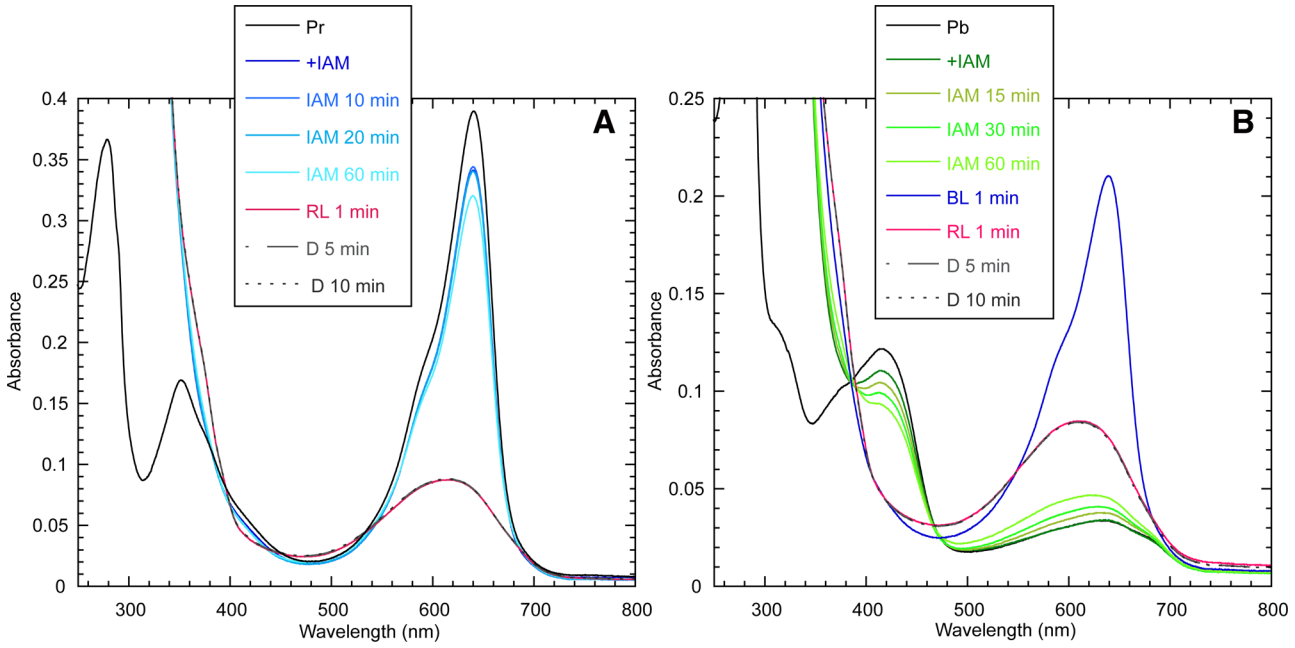

Figure 3. Iodoacetamide (final concentration of 50 mM) was added to a solution of (A) AM1_1186g2 Pr or (B) Pb. (A) Spectra of an AM1_1186g2 Pr solution immediately before (Pr) and immediately after addition of IAM (+IAM) and 10, 20, and 60 min after addition of IAM are shown. Spectra recorded after a 1 min red light irradiation of a Pr solution for Pr-to-Io photoconversion (RL 1 min) and after 5 and 10 min in the dark (D 5 min and D 10 min, respectively). (B) Spectra of an AM1_1186g2 Pb solution immediately before (Pb) and immediately after addition of IAM (+IAM) and 15, 30, and 60 min after addition of IAM are shown. Spectra recorded after a 1 min blue light irradiation of a Pb solution for Pb-to-Pr photoconversion (BL 1 min), after red light irradiation of a Pr solution for Pr-to-Io photoconversion (RL 1 min), and after 5 and 10 min in the dark (D 5 min and D 10 min, respectively).

Information)]. Cys2529 corresponds to the canonical Cys that stably binds ring A. We mapped the other three cysteines onto the AnPixJg2 Pr structure according to their sequence homologies (Figure 1 of the Supporting Information and Figure 4A).[24] Only Cys2510 is positioned next to the C ring of PCB, whereas Cys2460 and Cys2580 are too far from the chromophore to interact with it (Figure 4A). Given these observations, we first replaced Cys2460 and Cys2580 with alanines to form AM1_1186g2_CCAA, which we purified as the Pr dark state. Photoconversion of this form yielded the Pb photoproduct via formation of the Io intermediate in a manner similar to that of wild type AM1_1186g2, indicating that these two cysteines are not involved in the thiol-based photocycle (Figure 2 of the Supporting Information). Next, we replaced Cys2510 with an alanine to form AM1_1186g2_CA, which was purified in the dark as Pr for which its absorbance spectrum had a peak at 642 nm (Figure 4B). The spectral shapes, peak positions, and absorbance coefficients of the AM1_1186g2_CA and wild type Pr states are almost identical, strongly indicating that Cys2510 is not necessary for Pr formation (Figures 1D and 4B). AM1_1186g2_CA covalently bound PCB as shown by its zinc-dependent fluorescence (Figure 1C) and the absorbance spectrum of its denatured state (Figures 1C and 4C). Red light irradiation of AM1_1186g2_CA Pr led to the formation of Io, but conversion of Io to Pb did not occur in the dark by 10 min (Figure 4B). The spectra of acid-denatured AM1_1186g2_CA Pr and Io indicate that they contain 15*Z*-PCB and 15*E*-PCB, respectively (Figure 4C,D). In conclusion, Cys2510 transiently forms a covalent bond with PCB in Pb but not in Pr. Furthermore, the blue light-absorbing nature of Pb suggests that Cys2510 attaches to C10 of the chromophore as do other dual-Cys CBCRs.

Reaction Cycle. Although AM1_1186g2 can be classified as an R/G CBCR given its sequence (Figure 1 of the Supporting Information) and its position on the phylogenetic cluster (Figure 1B), it exhibits an unusual reversible photoconversion involving Pr with an absorbance maximum at 641 nm and Pb with an absorbance maximum at 416 nm. Its Pr-to-Pb photoconversion requires at least two steps (Figure 5). The intermediate Io is formed from red light-illuminated Pr with the transition involving a C15 *Z*/*E* isomerization of PCB, whereas the transition from Io to Pb involves the formation of a covalent bond between the thiol of Cys2510 and PCB in the dark (Figure 5). Conversely, the Pb-to-Pr conversion occurs quickly with first an *E*/*Z* isomerization and then detachment of Cys2510 from PCB (Figure 5). The peak wavelengths, spectral shapes, chromophore configurations, and stabilities in the dark of AM1_1186g2 and AnPixJg2 Pr are similar. Moreover, the spectral properties of Io are similar to those of the AnPixJg2 intermediate $R2_{610}$.[27,31] These observations suggest that AM1_1186g2 and AnPixJg2 share an initial common reaction mechanism for the formation of an intermediate but then diverge to form Pb and Pg, respectively.

Unique Photochemical Characteristics of AM1_1186g2. Most Cys adduct forms of dual-Cys CBCRs, i.e., B/G CBCRs and the insert-Cys CBCR VO1 (NpF2164g3), are stable in the dark, whereas their photoproducts are Cys-free states.[7,14,15,21,22] Only one B/G CBCR, NpR5313g2, is in the Pg state in the dark when Cys-free and in the Pb photoproduct state as a Cys adduct.[14] Because, as we have shown, the AM1_1186g2 Pr dark state is Cys-free and its Pb photoproduct is a Cys adduct, the AM1_1186g2 photocycle is, in some manner, similar to that of NpR5313g2. Namely, both AM1_1186g2 and NpR5313g2 have a Cys-free dark state, although the wavelength maximum of AM1_1186g2 Pr (641

dx.doi.org/10.1021/bi500376b | *Biochemistry* 2014, 53, 5051−5059

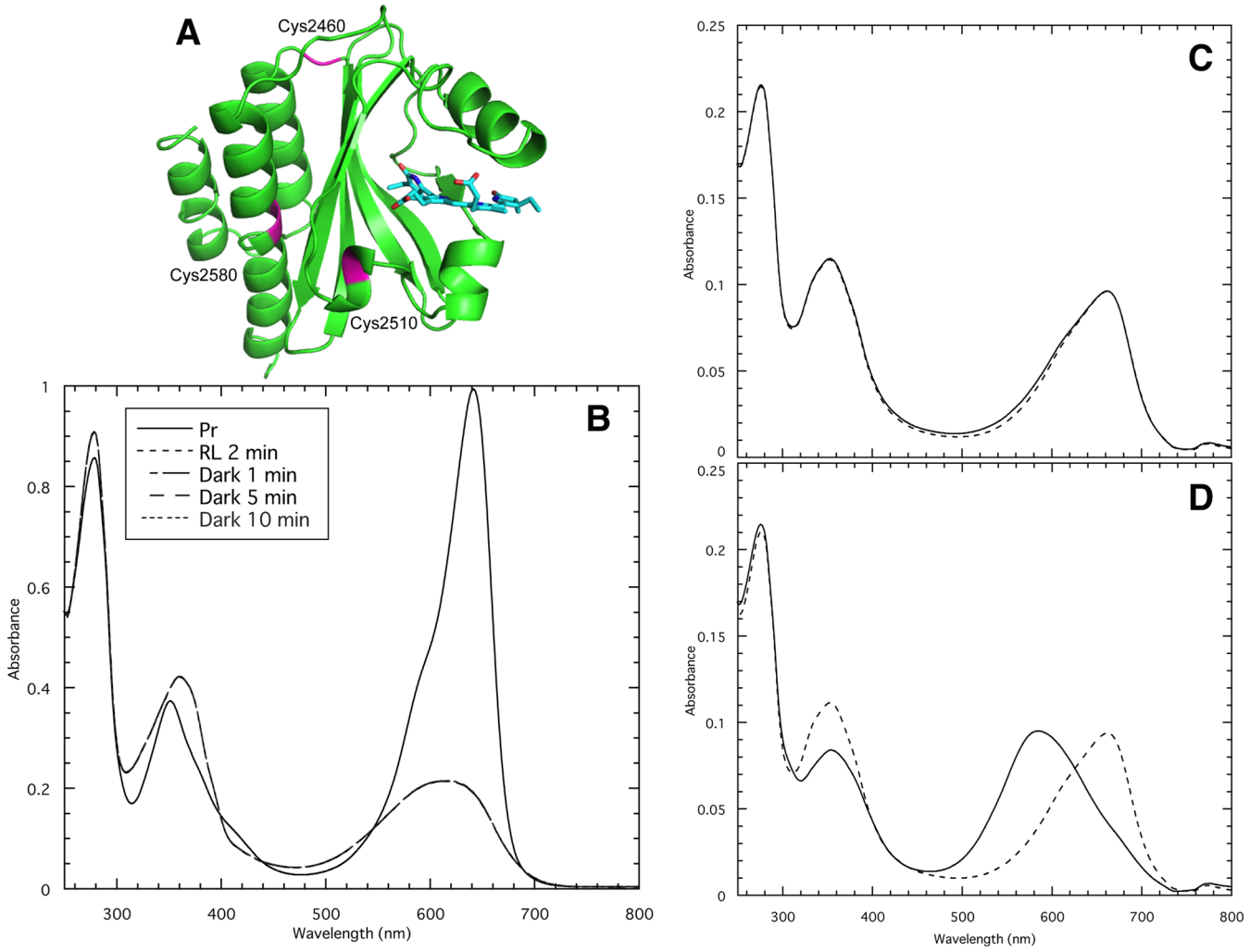

Figure 4. (A) Positions of AM1_1186g2 cysteines mapped onto an AnPixJg2 Pr ribbon diagram. The chromophore and cysteines are colored cyan and pink, respectively. (B) Spectra of an AM1_1186g2_CA Pr solution immediately before (Pr) and immediately after (RL 2 min) and 1, 5, and 10 min after red light illumination in the dark showing that AM1_1186g2_CA can photoconvert to Io but not to Pb. (C and D) Acid-denatured spectra of AM1_1186g2_CA Pr and AM1_1186g2_CA Io, respectively. Spectra were recorded immediately after denaturation (—) and after white light illumination (---).

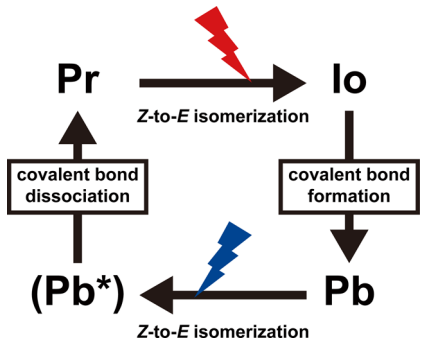

Figure 5. Reaction scheme for the photoconversion of AM1_1186g2. The Pr-to-Pb photoconversion occurs in two steps: a rapid *Z*/*E* isomerization of the C15═C16 bond followed by the slow formation of a covalent bond between Cys2510 and C10 of PCB. Conversely, the Pb-to-Pr photoconversion involves *E*/*Z* isomerization of the C15═C16 bond followed by rapid dissociation of the Cys2510−PCB covalent bond.

nm) is substantially red-shifted in comparison with that of NpR5313f2 Pg (550 nm). For NpR5313g2, Pg has been suggested to be deprotonated, resulting in the blue-shifted absorption.[14] However, because AM1_1186g2 Pr is quite similar to R/G AnPixJg2, AM1_1186g2 Pr is very likely to be protonated as is AnPixJg2 Pr, resulting in the red-shifted absorption.[33] In addition, because the second cysteine is involved in PVB formation and attached to the chromophore in the dark state in B/G CBCRs other than NpR5313g2, site-directed mutagenesis is not appropriate for clear proof of transient bond formation between a cysteine and PVB. In this context, because the Cys-free AM1_1186g2 Pr is the dark state and the chromophore is not PVB but PCB, IAM modification and site-directed mutagenesis provided sufficient evidence of the participation of the second cysteine during covalent bond formation. There has been no such report for NpR5313g2.

The wavelength separation of the peak maxima for AM1_1186g2 Pr and Pb is 225 nm, which is the largest known separation for two forms of a CBCR. The wavelength separations of the two forms of the dual-Cys phytochromes, TP1 and CparGPS1, are also extremely large, i.e., 278 and 258 nm, respectively.[6,7] Because only a GAF domain is needed for chromophore ligation and fully reversible photoconversion of CBCRs, whereas phytochromes require a much larger protein

dx.doi.org/10.1021/bi500376b | *Biochemistry* 2014, 53, 5051−5059

for photoconversion, AM1_1186g2 may find use in such applications as optogenetics.

The AM1_1186g2 Pr-to-Pb photoconversion consists of two steps: a *Z*/*E* photoisomerization followed by the slower formation of a covalent bond between Cys2510 and C10. Because this second step is temperature-dependent (Figure 2B), it may require protein flexibility. No other dual-Cys photoreceptors have been shown to exhibit slow formation of a covalent bond. Cys2510 does not correspond to known second cysteine resides according to our sequence alignment (Figure 1 of the Supporting Information). Thus, the unique positioning of Cys2510 may control the slow formation of the covalent bond.

Structural Insights into the AM1_1186g2 Photocycle. We have shown that Cys2510 in AM1_1186g2 very likely forms a covalent bond with C10 of PCB in Pb. Because AM1_1186g2 is quite similar to AnPixJg2 in sequence (42% identical), we predicted the AM1_1186g2 Pr structure by mapping its sequence onto the AnPixJg2 Pr structure.[24] Cys2510 of AM1_1186g2 corresponds to Tyr302 of AnPixJg2 in the primary sequence (Figure 6A). This Tyr302 is located 7−8 Å from C10 of PCB in the AnPixJg2 Pr structure (Figure 3 of the Supporting Information). Notably, there are many nonconserved residues near these Tyr302 and Cys2510 residues (Figure 6A). In particular, Arg301 upstream of Tyr302 is replaced with Pro2501 in AM1_1186g2. Arg301 in AnPixJg2 is hydrogen bonded to the stretched C8 propionate of PCB (Figure 3 of the Supporting Information). In AM1_1186g2, however, Pro2519 may distort the local protein structure to allow transient adduct formation. To examine role of Pro2509 in the AM1_1186g2 photocycle, we replaced Pro2509 with an alanine to form AM1_1186g2_PA, which showed a red/blue reversible photoconversion without noticeable accumulation of Io (Figure 6B), indicating perhaps that a structural arrangement induced by Pro2509 is critical for the slow generation of Pb. Furthermore, because mutation of Cys2510 to an alanine resulted in the arrest at Io but no Pg formation, in addition to Cys2510, other nearby residues, including Pro2509, should be involved in the unique red/blue reversible photochemistry of AM1_1186g2.

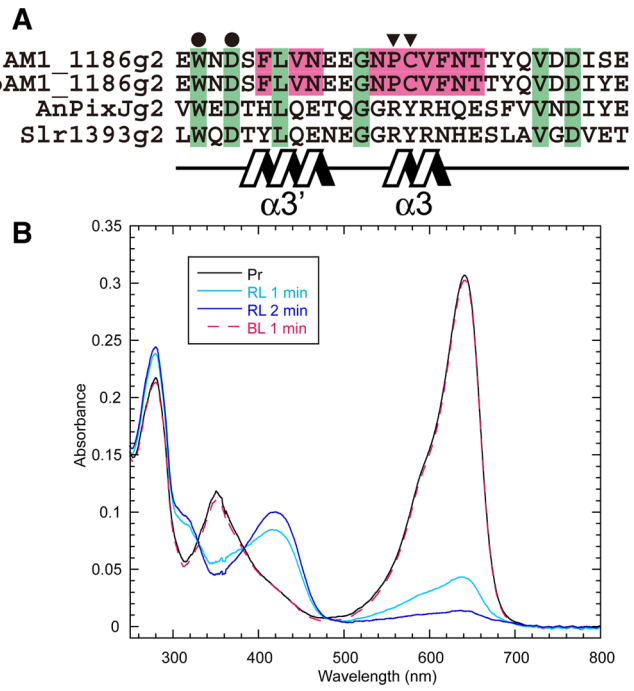

Figure 6. (A) Residues in helices α3 and α3′ of AM1_1186g2, oAM1_1186g2 (orthologous GAF domain from *Acaryochloris* sp. CCMEE5410), AnPixJg2, and Slr1393g2. Arrowheads identify Cys2510 that is bound to PCB in AM1_1186g2 Pb and Pro2509, which is important for the rate of cysteinylation. Circles identify Trp2497 and Asp2499 that are suggested to be involved in signal transduction during AnPixJg2 photoconversion. Conserved AM1_1186g2 and oAM1_1186g2 residues are highlighted in pink. Residues highlighted in green are conserved in the four CBCR GAF domains. (B) Spectra of an AM1_1186g2_PA Pr solution immediately before (Pr) and immediately after 1 and 2 min red light irradiations (RL 1 min and RL 2 min, respectively) and after a 1 min blue light irradiation (BL 1 min).

However, tryptophan and aspartate (Trp2497 and Asp2499 in AM1_1186g2) that were suggested to be involved in signal transduction during the initial AnPixJg2 photoconversion are conserved in AM1_1186g2 (Figure 6A). Any structural changes involving these residues may facilitate a conformational rearrangement of ring A and the surrounding AnPixJg2 residues, which may also be important for AM1_1186g2 Pb formation.

Plasticity and Evolutionary Flexibility of CBCRs. It is quite interesting that AM1_1186g2 emerged from R/G CBCRs (Figure 1B) as did insert-Cys CBCRs. Although B/G and insert-Cys CBCRs possess a cysteine that reversibly binds C10 of the chromophore, the cysteines are evolutionarily distinctive according to our sequence alignment (Figure 1 of the Supporting Information). At present, a number of sequentially different types of dual-Cys CBCRs and phytochromes have been reported: B/G CBCRs with a DXCF motif,[14] insert-Cys CBCRs,[7] dual-Cys phytochromes,[6,7] AM1_1186g2 as reported herein, and perhaps GwitGPS1. Interestingly, the positions of the second cysteine differ for these photoreceptors (Figure 1 of the Supporting Information), indicating that they emerged independently during evolution. Further, the structural positions of the second cysteines also differ. For the purpose of the following discussion, we define the protein structure next to the α-face of the chromophore as the upper face and the one next to the β-face as the lower face, using the definitions of a previous study.[16] The covalently bound second cysteines of the B/G CBCRs and dual-Cys phytochromes are found on the lower and upper faces, respectively.[23,25,42] Cys2510 of AM1_1186g2 should be located near the lower face judging from the mapping analysis (Figure 3 of the Supporting Information), which would be a position similar to those of the B/G CBCR cysteine. Because the positioning of the second cysteine has built-in flexibility, color tuning by the second cysteine may be more promiscuous than previously recognized.

Although we searched orthologous domains of AM1_1186g2 against a nonredundant database and a microbial genome database of NCBI, an orthologous domain was detected only from very related species *Acaryochloris* sp. CCMEE5410. This orthologous domain also possesses the second Cys residue, suggesting similar red/blue photoconversion (Figure 6A). Because other cyanobacteria do not possess this type of GAF domain, these domains are likely to have emerged only within *Acaryochloris*. AM1_1186 is an extremely large protein that contains many different functional domains, with sequences homologous to others from cyanobacteria.[43,44] These proteins share the same minimal domain architecture: an N-terminal Ser/Thr kinase domain followed by a long conserved region of

dx.doi.org/10.1021/bi500376b | *Biochemistry* 2014, 53, 5051−5059

unknown function, a non-CBCR GAF domain, and a His-kinase domain. Interestingly, various Per/ARNT/Sim and GAF domains are often found between the non-CBCR GAF domain and His-kinase domain. These inserted domains are highly diverse in their kinds, numbers, and sequences,[43,44] suggesting that the region between the non-CBCR GAF domain and the His-kinase domain is a hot spot for domain shuffling and evolution and that AM1_1186g2 is a product of evolutionary flexibility.

■ ASSOCIATED CONTENT

Supporting Information

Multiple-sequence alignment of CBCR and phytochrome GAF domains; spectra of AM1_1886g2_CCAA Pr, Io, and Pb; and structure of AnPixJg2 Pr near rings B and C. This material is available free of charge via the Internet at http://pubs.acs.org.

■ AUTHOR INFORMATION

Corresponding Author

*E-mail: narikawa.rei@shizuoka.ac.jp. Telephone: +81-54-238-4783.

Funding

This work was supported by JST, PRESTO (to R.N.), Grants-in-Aid for Young Scientists (to R.N.), and Grants-in-Aid for Scientific Research (to M.I.).

Notes

The authors declare no competing financial interest.

■ ABBREVIATIONS

B/G, blue/green; CBCR, cyanobacteriochrome; IAM, iodoacetamide; Io, intermediate that absorbs orange light; SDS−PAGE, sodium dodecyl sulfate−polyacrylamide gel electrophoresis; Pb, blue light-absorbing form; PCB, phycocyanobilin; Pg, green light-absorbing form; Pr, red light-absorbing form; PVB, phycoviolobilin; R/G, red/green.

■ REFERENCES

(1) Franklin, K. A., and Quail, P. H. (2010) Phytochrome functions in *Arabidopsis* development. *J. Exp. Bot. 61*, 11−24.

(2) Rockwell, N. C., and Lagarias, J. C. (2010) A brief history of phytochromes. *ChemPhysChem 11*, 1172−1180.

(3) Auldridge, M. E., and Forest, K. T. (2011) Bacterial phytochromes: More than meets the light. *Crit. Rev. Biochem. Mol. Biol. 46*, 67−88.

(4) Ulijasz, A. T., and Vierstra, R. D. (2011) Phytochrome structure and photochemistry: Recent advances toward a complete molecular picture. *Curr. Opin. Plant Biol. 14*, 498−506.

(5) Hughes, J. (2010) Phytochrome three-dimensional structures and functions. *Biochem. Soc. Trans. 38*, 710−716.

(6) Rockwell, N. C., Duanmu, D., Martin, S. S., Bachy, C., Price, D. C., Bhattacharya, D., Worden, A. Z., and Lagarias, J. C. (2014) Eukaryotic algal phytochromes span the visible spectrum. *Proc. Natl. Acad. Sci. U.S.A. 111*, 3871−3876.

(7) Rockwell, N. C., Martin, S. S., Feoktistova, K., and Lagarias, J. C. (2011) Diverse two-cysteine photocycles in phytochromes and cyanobacteriochromes. *Proc. Natl. Acad. Sci. U.S.A. 108*, 11854−11859.

(8) Ikeuchi, M., and Ishizuka, T. (2008) Cyanobacteriochromes: A new superfamily of tetrapyrrole-binding photoreceptors in cyanobacteria. *Photochem. Photobiol. Sci. 7*, 1159−1167.

(9) Savakis, P., De Causmaecker, S., Angerer, V., Ruppert, U., Anders, K., Essen, L. O., and Wilde, A. (2012) Light-induced alteration of c-di-GMP level controls motility of *Synechocystis* sp. PCC 6803. *Mol. Microbiol. 85*, 239−251.

(10) Song, J. Y., Cho, H. S., Cho, J. I., Jeon, J. S., Lagarias, J. C., and Park, Y. I. (2011) Near-UV cyanobacteriochrome signaling system elicits negative phototaxis in the cyanobacterium *Synechocystis* sp. PCC 6803. *Proc. Natl. Acad. Sci. U.S.A. 108*, 10780−10785.

(11) Narikawa, R., Suzuki, F., Yoshihara, S., Higashi, S., Watanabe, M., and Ikeuchi, M. (2011) Novel photosensory two-component system (PixA-NixB-NixC) involved in the regulation of positive and negative phototaxis of cyanobacterium *Synechocystis* sp. PCC 6803. *Plant Cell Physiol. 52*, 2214−2224.

(12) Hirose, Y., Narikawa, R., Katayama, M., and Ikeuchi, M. (2010) Cyanobacteriochrome CcaS regulates phycoerythrin accumulation in *Nostoc punctiforme*, a group II chromatic adapter. *Proc. Natl. Acad. Sci. U.S.A. 107*, 8854−8859.

(13) Bussell, A. N., and Kehoe, D. M. (2013) Control of a four-color sensing photoreceptor by a two-color sensing photoreceptor reveals complex light regulation in cyanobacteria. *Proc. Natl. Acad. Sci. U.S.A. 110*, 12834−12839.

(14) Rockwell, N. C., Martin, S. S., Gulevich, A. G., and Lagarias, J. C. (2012) Phycoviolobilin formation and spectral tuning in the DXCF cyanobacteriochrome subfamily. *Biochemistry 51*, 1449−1463.

(15) Enomoto, G., Hirose, Y., Narikawa, R., and Ikeuchi, M. (2012) Thiol-based photocycle of the blue and teal light-sensing cyanobacteriochrome Tlr1999. *Biochemistry 51*, 3050−3058.

(16) Rockwell, N. C., Njuguna, S. L., Roberts, L., Castillo, E., Parson, V. L., Dwojak, S., Lagarias, J. C., and Spiller, S. C. (2008) A second conserved GAF domain cysteine is required for the blue/green photoreversibility of cyanobacteriochrome Tlr0924 from *Thermosynechococcus elongatus*. *Biochemistry 47*, 7304−7316.

(17) Ishizuka, T., Shimada, T., Okajima, K., Yoshihara, S., Ochiai, Y., Katayama, M., and Ikeuchi, M. (2006) Characterization of cyanobacteriochrome TePixJ from a thermophilic cyanobacterium *Thermosynechococcus elongatus* strain BP-1. *Plant Cell Physiol. 47*, 1251−1261.

(18) Yoshihara, S., Katayama, M., Geng, X., and Ikeuchi, M. (2004) Cyanobacterial phytochrome-like PixJ1 holoprotein shows novel reversible photoconversion between blue- and green-absorbing forms. *Plant Cell Physiol. 45*, 1729−1737.

(19) Ma, Q., Hua, H. H., Chen, Y., Liu, B. B., Kramer, A. L., Scheer, H., Zhao, K. H., and Zhou, M. (2012) A rising tide of blue-absorbing biliprotein photoreceptors: Characterization of seven such bilin-binding GAF domains in *Nostoc* sp. PCC7120. *FEBS J. 279*, 4095−4108.

(20) Ishizuka, T., Narikawa, R., Kohchi, T., Katayama, M., and Ikeuchi, M. (2007) Cyanobacteriochrome TePixJ of *Thermosynechococcus elongatus* harbors phycoviolobilin as a chromophore. *Plant Cell Physiol. 48*, 1385−1390.

(21) Rockwell, N. C., Martin, S. S., and Lagarias, J. C. (2012) Mechanistic insight into the photosensory versatility of DXCF cyanobacteriochromes. *Biochemistry 51*, 3576−3585.

(22) Ishizuka, T., Kamiya, A., Suzuki, H., Narikawa, R., Noguchi, T., Kohchi, T., Inomata, K., and Ikeuchi, M. (2011) The cyanobacteriochrome, TePixJ, isomerizes its own chromophore by converting phycocyanobilin to phycoviolobilin. *Biochemistry 50*, 953−961.

(23) Cornilescu, C. C., Cornilescu, G., Burgie, E. S., Markley, J. L., Ulijasz, A. T., and Vierstra, R. D. (2014) Dynamic Structural Changes Underpin Photoconversion of a Blue/Green Cyanobacteriochrome between Its Dark and Photoactivated States. *J. Biol. Chem. 289*, 3055−3065.

(24) Narikawa, R., Ishizuka, T., Muraki, N., Shiba, T., Kurisu, G., and Ikeuchi, M. (2013) Structures of cyanobacteriochromes from phototaxis regulators AnPixJ and TePixJ reveal general and specific photoconversion mechanism. *Proc. Natl. Acad. Sci. U.S.A. 110*, 918−923.

(25) Burgie, E. S., Walker, J. M., Phillips, G. N., Jr., and Vierstra, R. D. (2013) A photo-labile thioether linkage to phycoviolobilin provides the foundation for the blue/green photocycles in DXCF-cyanobacteriochromes. *Structure 21*, 88−97.

(26) Gottlieb, S. M., Kim, P. W., Corley, S. C., Madsen, D., Hanke, S. J., Chang, C. W., Rockwell, N. C., Martin, S. S., Lagarias, J. C., and Larsen, D. S. (2014) Primary and secondary photodynamics of the

violet/orange dual-cysteine NpF2164g3 cyanobacteriochrome domain from *Nostoc punctiforme*. *Biochemistry 53*, 1029−1040.
(27) Narikawa, R., Fukushima, Y., Ishizuka, T., Itoh, S., and Ikeuchi, M. (2008) A novel photoactive GAF domain of cyanobacteriochrome AnPixJ that shows reversible green/red photoconversion. *J. Mol. Biol. 380*, 844−855.
(28) Kim, P. W., Freer, L. H., Rockwell, N. C., Martin, S. S., Lagarias, J. C., and Larsen, D. S. (2012) Second-chance forward isomerization dynamics of the red/green cyanobacteriochrome NpR6012g4 from *Nostoc punctiforme*. *J. Am. Chem. Soc. 134*, 130−133.
(29) Kim, P. W., Freer, L. H., Rockwell, N. C., Martin, S. S., Lagarias, J. C., and Larsen, D. S. (2012) Femtosecond photodynamics of the red/green cyanobacteriochrome NpR6012g4 from *Nostoc punctiforme*. 1. Forward dynamics. *Biochemistry 51*, 608−618.
(30) Kim, P. W., Freer, L. H., Rockwell, N. C., Martin, S. S., Lagarias, J. C., and Larsen, D. S. (2012) Femtosecond photodynamics of the red/green cyanobacteriochrome NpR6012g4 from *Nostoc punctiforme*. 2. reverse dynamics. *Biochemistry 51*, 619−630.
(31) Fukushima, Y., Iwaki, M., Narikawa, R., Ikeuchi, M., Tomita, Y., and Itoh, S. (2011) Photoconversion mechanism of a green/red photosensory cyanobacteriochrome AnPixJ: Time-resolved optical spectroscopy and FTIR analysis of the AnPixJ-GAF2 domain. *Biochemistry 50*, 6328−6339.
(32) Chen, Y., Zhang, J., Luo, J., Tu, J. M., Zeng, X. L., Xie, J., Zhou, M., Zhao, J. Q., Scheer, H., and Zhao, K. H. (2012) Photophysical diversity of two novel cyanobacteriochromes with phycocyanobilin chromophores: Photochemistry and dark reversion kinetics. *FEBS J. 279*, 40−54.
(33) Velazquez Escobar, F., Utesch, T., Narikawa, R., Ikeuchi, M., Mroginski, M. A., Gartner, W., and Hildebrandt, P. (2013) Photoconversion mechanism of the second GAF domain of cyanobacteriochrome AnPixJ and the cofactor structure of its green-absorbing state. *Biochemistry 52*, 4871−4880.
(34) Narikawa, R., Muraki, N., Shiba, T., Ikeuchi, M., and Kurisu, G. (2009) Crystallization and preliminary X-ray studies of the chromophore-binding domain of cyanobacteriochrome AnPixJ from *Anabaena* sp. PCC 7120. *Acta Crystallogr. F65*, 159−162.
(35) Rockwell, N. C., Martin, S. S., Gulevich, A. G., and Lagarias, J. C. (2014) Conserved phenylalanine residues are required for blue-shifting of cyanobacteriochrome photoproducts. *Biochemistry 53*, 3118−3130.
(36) Schultz, J., Milpetz, F., Bork, P., and Ponting, C. P. (1998) SMART, a simple modular architecture research tool: Identification of signaling domains. *Proc. Natl. Acad. Sci. U.S.A. 95*, 5857−5864.
(37) Thompson, J. D., Gibson, T. J., Plewniak, F., Jeanmougin, F., and Higgins, D. G. (1997) The CLUSTAL_X windows interface: Flexible strategies for multiple sequence alignment aided by quality analysis tools. *Nucleic Acids Res. 25*, 4876−4882.
(38) Huson, D. H., Richter, D. C., Rausch, C., Dezulian, T., Franz, M., and Rupp, R. (2007) Dendroscope: An interactive viewer for large phylogenetic trees. *BMC Bioinf. 8*, 460.
(39) Mukougawa, K., Kanamoto, H., Kobayashi, T., Yokota, A., and Kohchi, T. (2006) Metabolic engineering to produce phytochromes with phytochromobilin, phycocyanobilin, or phycoerythrobilin chromophore in *Escherichia coli*. *FEBS Lett. 580*, 1333−1338.
(40) Berkelman, T. R., and Lagarias, J. C. (1986) Visualization of bilin-linked peptides and proteins in polyacrylamide gels. *Anal. Biochem. 156*, 194−201.
(41) Hansen, R. E., and Winther, J. R. (2009) An introduction to methods for analyzing thiols and disulfides: Reactions, reagents, and practical considerations. *Anal. Biochem. 394*, 147−158.
(42) Essen, L. O., Mailliet, J., and Hughes, J. (2008) The structure of a complete phytochrome sensory module in the Pr ground state. *Proc. Natl. Acad. Sci. U.S.A. 105*, 14709−14714.
(43) Narikawa, R., Okamoto, S., Ikeuchi, M., and Ohmori, M. (2004) Molecular evolution of PAS domain-containing proteins of filamentous cyanobacteria through domain shuffling and domain duplication. *DNA Res. 11*, 69−81.
(44) Fujisawa, T., Narikawa, R., Okamoto, S., Ehira, S., Yoshimura, H., Suzuki, I., Masuda, T., Mochimaru, M., Takaichi, S., Awai, K., Sekine, M., Horikawa, H., Yashiro, I., Omata, S., Takarada, H., Katano, Y., Kosugi, H., Tanikawa, S., Ohmori, K., Sato, N., Ikeuchi, M., Fujita, N., and Ohmori, M. (2010) Genomic structure of an economically important cyanobacterium, *Arthrospira* (*Spirulina*) *platensis* NIES-39. *DNA Res. 17*, 85−103.